**The Canadian Society for Bioengineering**
*The Canadian society for engineering in agricultural, food, environmental, and biological systems*.

CSBE | SCGAB

**La Société Canadienne de Génie Agroalimentaire et de Bioingénierie**
*La société canadienne de génie agroalimentaire, de la bioingénierie et de l'environnement*

**Paper No. 06-155S**

# An Exploration Strategy for Autonomous Construction of Agricultural Field Maps

**L. Liu, T.G. Crowe, and M. Roberge**
Department of Agricultural & Bioresource Engineering, University of Saskatchewan
57 Campus drive, Saskatoon, Saskatchewan, Canada, S7N 5A9

**Written for presentation at the**
**CSBE/SCGAB 2006 Annual Conference**
**Edmonton Alberta**
**July 16 - 19, 2006**

## ABSTRACT

This paper addresses the automatic mapping problem of moving an image sensor to collect the terrain information and concomitantly construct a terrain map while circumventing obstacles in the working field. A terrain map is incrementally built by image sensor readings. At each step, the robot decides where to go to collect new terrain information based on a partially-built map.

In this work, a triangular mesh map was used to represent the agricultural field surface due to its efficiency to represent large rough areas. A 3D image sensor model, with attributes similar to a camera or laser sensor, was used in the simulation. This paper presents the concept of including energy consumption within the cost function to choose the next-best view. The cost function not only considers the traveling distance, but also includes energy required to change elevation, the rolling resistance of the terrain and vehicle tire slip during exploration. This exploration strategy was validated by simulation. The results show the effectiveness of the minimum energy cost to choose the next-best-view point in the exploration task. **Keywords:** Robotics, Autonomous exploration, Map building, Terrain Modeling, Next-best-view, Precision agriculture.

## 1. INTRODUCTION

An agricultural vehicle equipped with an automatic guidance system could help to alleviate the farming labor shortage problem and inspire the use of selective chemical application. Research efforts have concentrated on guiding the vehicle by finding a path from landmarks such as crop rows and furrows in an agricultural field (Åstrand and Baerveldt 2002; Keicher and Seufert 2000; Nielsen et al. 2002; Ollis and Stentz 1996; Reid and Searcy 1987; Reid et al. 2000; Tillett and Hague 1999). For vehicle guidance in a large unstructured agricultural field, one problem will involve providing a high-resolution terrain map with detailed information about the obstacles in the field for task planning.

This paper addresses the automatic mapping problem of moving an image sensor to collect the terrain information and concomitantly construct a terrain map while circumventing obstacles in the working field. A terrain map is incrementally built by image sensor readings. At each step, the robot decides where to go to collect new information based on a partially-built map. This is a typical *next-best-view* problem (Gonzalez-Banos and Latombe 2002) in robotic exploration.

Several exploration strategies have been developed to address autonomous construction of maps. One group of approaches utilizes pattern paths to explore the whole field. These algorithms (Choset 2001; Hert et al. 1996; Huang 2001) take the following basic approach to generate a coverage path: the region to be covered is decomposed into subregions, a traveling-salesman algorithm (Choset 2001) is applied to generate a sequence of subregions to visit, and a coverage path is generated from this sequence that covers each subregion in turn. All of these algorithms use a single line sweep in order to decompose the coverage region into subregions, and these subregions are individually covered using a back and forth motion in rows perpendicular to the sweep direction. The limitation of this group of strategies is that the efficiency of these approaches is heavily affected by the line sweeping direction. Another group of exploration strategies is to choose a next-best-view point among frontiers (Yamauchi 1997) extracted from the boundary between the known and unknown areas. Path distance is typically used in the cost function to select the next-best-view point for the robot to move to explore new terrain (Gonzalez-Banos and Latombe 2002; Sujan and Dubowsky 2005; Taylor and Kriegman 1998; Thrun et al. 1998; Yamauchi 1997). However, to explore agricultural fields, the problem is complicated by a number of farming issues. One of the most important issues is that agricultural field surfaces are usually rough. Travel distance alone is unsuitable to represent traveling cost in the rough terrain of an outdoor unstructured environment. The ruggedness of terrain influences the exploration strategy employed by a robot because the cost of driving is not the same for all traversable areas.

This paper presents the concept of including energy consumption within the cost function to choose the next-best-view point. The cost function not only considers the traveling distance, but also includes energy required to change elevation, the rolling resistance of the terrain and vehicle tire slip during exploration.

## 2. WORLD MODEL

This research was initiated to design an algorithm that would guide a mobile robot to explore and map large unstructured rough agricultural fields. Two-dimensional polygonal maps which have been extensively used in planar environments (Bourgault et al. 2002; Stachniss and Burgard 2003; Taylor and Kriegman 1998) are definitely not suitable to represent three-dimensional rough agricultural fields. Some research (Moorehead et al. 2001; Sujan and Dubowsky 2005; Thrun et al. 2005) described 3D grid maps for representation of 3D outdoor environments. However grid maps will become intractable for a large-size agricultural field. Dupuis et al. (2004) used the triangular mesh map to represent a Mars-like environment in a planetary exploration task. The triangular mesh map is proposed in this research to model the agricultural field surface because of its efficacy in representing large-size environments, such as rough agricultural fields. The triangular mesh map also has advantages over grid maps in its ability to generate a smoother path for navigation tasks. Every triangle has 3 edge neighbors and 9 vertex neighbors, so it has 12 cell neighbors in a non-boundary triangle cell. The triangle mesh map provides 12 moving direction choices for each location, which results in a much smoother path compared with the traditional grid map.

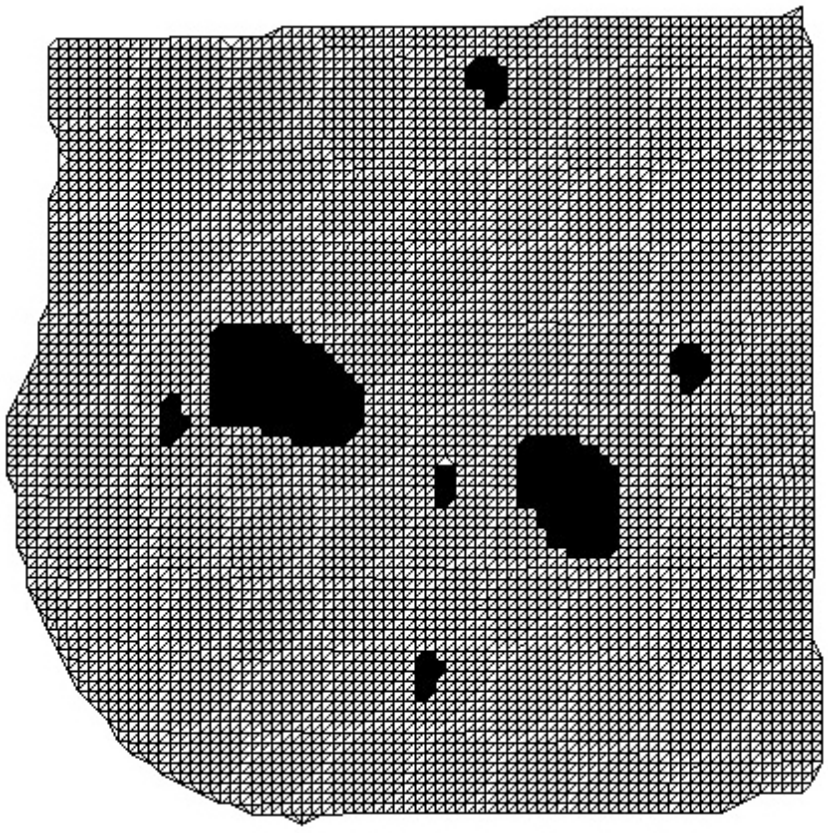

Figure 1. Triangular mesh map of an agricultural field environment (black blobs represent obstacles).

The triangular mesh map is incrementally built by laser sensor readings based on Delaunay triangulation (Schroeder et al. 1996). The Visualization Toolkits (Kitware Inc. 2005), available freely on the World Wide Web, has been used to implement the

triangulation in this simulation. Figure 1 is the triangular mesh map of an agricultural field. The triangular mesh map is stored in the computer as a directed weighted graph; the vertex of which is used to represent every triangle, and the edge represents the relative difficulty to traverse the adjacent triangle.

## 3. IMAGE SENSOR MODEL

Most coverage and exploration algorithms include ideal sensors. The assumption is that if the robot traverses a cell, then the whole cell is covered (Moorehead et al. 2001). Very few researchers have investigated the exploration algorithm with 3D real image sensors. To account for challenges associated with rough terrain and incomplete visibility, where one part of the terrain may occlude other parts, a 3D view model was used.

### 3.1 Frustum culling

The image sensor's capacity is constrained by its pose (position and orientation), field of view (angles between the left and right sides and top and bottom sides of the viewing capacity), and depth of field (sensor capacity in length, $Z_{near}$ and $Z_{far}$). The viewing frustum shown in Fig. 2 is defined by 6 planes, which are named the near, far, left, right, top and bottom planes. The viewing frustum defines the visibility of every triangle in the terrain for each viewpoint, and triangles inside the viewing frustum are visible to the user.

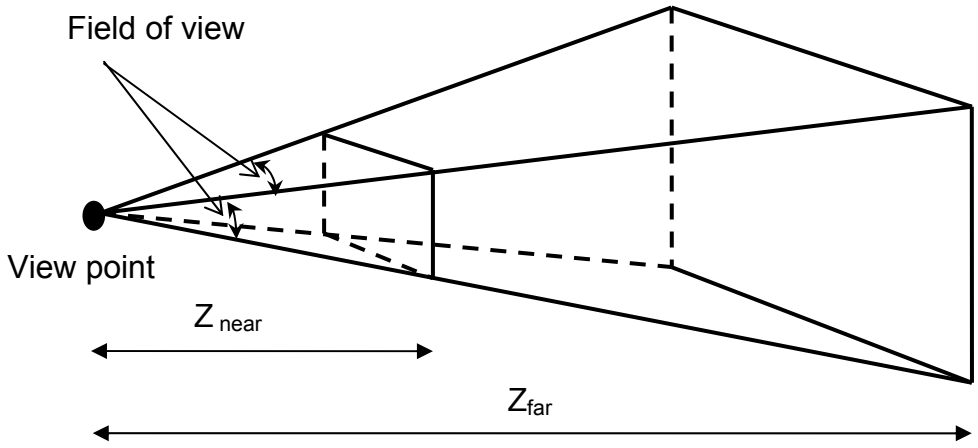


Figure 2. Image sensor viewing frustum.

### 3.2 Ray Casting Algorithm

For surface visibility calculations, the viewing frustum culling is used to clip the triangles bounded by the camera frustum in the first step. The next step is to check the visibility of every triangle contained in the frustum using a ray casting algorithm. The basic ray

casting algorithm involves throwing a lot of rays into the scene (Hearn 1994). The algorithm begins, as in ray casting, by shooting a ray from the view point and through the screen (far plane of the viewing frustum), Then, every element (triangle) inside the viewing frustum is tested to see if the given ray intersects any of them, and finding the nearest of those intersections to the view point. From the point of intersection (z depth), the triangle nearest to the view point is visible through this ray, while other elements which have intersection with the ray are shadowed. In this way the visible triangles can be identified as those which intersect contiguous rays with the shortest distance to the view point.

## 4. EXPLORATION ALGORITHM

The core of this research is to choose appropriate next-best-view points. Energy cost is critical in farming due to its economical impacts, so this paper proposes the concept of including energy consumption within the cost function to choose the next-best-view point. The goal of the exploration is to consume the minimum amount of energy to explore new terrain in each step. The energy cost function not only considers the traveling distance but also includes energy required to change elevation, the rolling resistance of the terrain and vehicle tire slip during exploration.

### 4.1 Energy cost function

Suvinen et al. (2003) proposed the concept of generating a cost surface based on machine, terrain, tree coverage, road and weather objects for GIS-based terrain mobility modeling and optimization of off-road routes. The energy cost function through a vehicle tractive function is derived below. The equation of motion along the longitudinal axis of the vehicle was expressed by Wong (1978) as

$$F_t = R_a + R_r + R_d + R_s + R_i, \quad (1)$$

where:

$F_t$ = the tractive effort (N),
$R_a$ = the aerodynamic resistance of the vehicle (N),
$R_r$ = the rolling resistance of the vehicle (N),
$R_d$ = the drawbar load (N),
$R_s$ = the slope resistance (N), and
$R_i$ = the inertial resistance (N).

Aerodynamic resistance is usually not a significant factor for off-road vehicles operating at speeds below 48 km/h (Wong 1978), and it is assumed as zero in this research. Drawbar pull $R_d$ was also assumed zero for exploration robots. When the velocity remains constant, inertial resistance, $R_i$, is zero. Slope resistance is calculated using the inclined plane equation,

$$R_s = W \sin\theta, \quad (2)$$

where W is the weight of the vehicle (N) and θ is the inclination angle of the terrain. When driving uphill (θ is positive), slope resistance is in the opposite direction of the vehicle's tractive force and it functions as a resistant force. When driving downhill (θ is negative), slope resistance is in the same direction of the vehicle's tractive force and the

slope resistance works as an active force.

On a slope at a constant low speed, the tractive effort, $F_t$, must overcome slope resistance and rolling resistance,

$$F_t = W * \sin\theta + R_r . \quad (3)$$

The rolling resistance of a pneumatic tire is dependent on load, size, tread pattern and inflation pressure, as well as soil strength (Liljedahl et al. 1989). For soils that are not very soft and tires with width/diameter ratio of approximately 0.3, along with tires deflection/section height ratio (δ/h) limitation of 0.20, the rolling resistance for a single tire can be predicted from

$$R_t = W_t(\frac{1.2}{C_n} + 0.04), \quad (4)$$

where:

$R_t$ = the rolling resistance for a single tire (N),

$C_n$ = $\frac{CI * b * d}{W_t}$, wheel numeric (dimensionless),

CI = cone index measured with a cone penetrometer as in ASAE S 313.2 ($N/cm^2$),

$W_t$ = $\frac{W\cos\theta}{4}$ for a 4WD vehicle with identical tires, load on a single tire (N),

b = the tire width (cm), and

d = the tire diameter (cm).

The total rolling resistance for a 4WD vehicle on a slope, with identical tires (b/d ≈ 0.3), along with a δ/h limitation of 0.20, the total rolling resistance of the vehicle can be predicted from

$$R_r = W\cos\theta(\frac{1.2}{C_n} + 0.04). \quad (5)$$

With the tractive force and the path length known, energy requirement of the vehicle traveling along a straight line path can be derived by

$$E = \frac{F_t * l}{1 - s}, \quad (6)$$

where:

E = the energy requirement (N m),

l = the Euclidean distance or the surface distance of the path (m),

s = $1 - \frac{V_a}{V_t}$, the wheel slip rate,

$V_a$ = actual travel speed (m/s), and

$V_t$ = theoretical wheel speed (m/s).

Substituting Eqs. 3 and 5 into Eq. 6, the energy requirement can be represented by

$$E = \frac{W}{1-s} * (l * \sin\theta + l * \cos\theta * (\frac{1.2}{C_n} + 0.04)). \quad (7)$$

Substituting the wheel numeric definition and trigonometric functions into Eq. 7,

$$E = \frac{W}{1-s} * (\Delta z + d_h(\frac{d_h}{l * CI} A + 0.04)), \quad (8)$$

where:

$\Delta z = l * \sin\theta$, slope height of the path (m),

$d_h = l * \cos\theta$, horizontal distance of the path (m), and

$A = \frac{0.3W}{b * d}$, constant (N/cm$^2$).

$\Delta z$ is positive on a uphill slope, while it is negative on a downward slope. In this paper, the maximum uphill slope is 30 degrees, limited by vehicle capabilities. Similarly, the maximum downhill slope is 35 degrees.

The total energy requirement for the vehicle to reach from a start location to destination is calculated by integration of energy in the piecewise path.

$$E_{total} = W * \sum_{i=1}^{n} [(\frac{1}{1-s_i}) * (\Delta z_i + d_{hi}(\frac{d_{hi}}{l_i * CI_i} * A + 0.04)], \quad (9)$$

where:

$E_{total}$ = total energy requirement (W h),

$\Delta z_i$ = the slope height of the $i_{th}$ segment of a piecewise path (m),

$d_{hi}$ = the horizontal distance of the $i_{th}$ segment of a piecewise path (m),

$n$ = the number of the segments of the path,

$s_i$ = the slip rate of the $i_{th}$ segment of a piecewise path,

$l_i$ = the Euclidean distance of the $i_{th}$ segment of a piecewise path (m), and

$CI_i$ = the cone index of the $i_{th}$ segments of the path (N/cm$^2$).

Assuming that soil hardness, $CI_i$, of the field is known and uniform, the energy requirement can by calculated by

$$E_{total} = W * \sum_{i=1}^{n} [(\frac{1}{1-s_i}) * (\Delta z_i + d_{hi} * \mu_i)], \quad (10)$$

where:

$\mu_i = \frac{d_{hi}}{l_i} * B + 0.04$, rolling resistance coefficient (dimensionless), and

$B = \frac{0.3W}{CI * b * d}$, constant (dimensionless).

The energy function, Eq. 10, shows that the energy consumption is proportional to the elevation change $\Delta z_i$. When driving uphill, $\Delta z_i$ is positive and slope resistance is in the opposite direction of the vehicle's tractive force. When driving downhill, $\Delta z_i$ is

negative and the slope resistance is in the same direction as the vehicle's tractive force. Assuming the vehicle travels at a constant speed in this paper, brake energy will be required when the negative elevation change, $\Delta z_i$, is excessive.

The energy consumption is also proportional to the horizontal trip distance of the vehicle. The contribution of travel distance to the energy consumption will vary considerably in relation to the rolling resistance coefficient, $\mu_i$. A tire's rolling resistance coefficient depends on the soil hardness as indicated by Cone index readings, terrain slope and wheel parameters. Load has a positive relationship with the energy in that the robot needs fuel to carry the load. Load also affects the energy by changing the magnitude of the rolling resistance coefficient. Slip between the tire and soil surface during exploration affects the energy consumption by generating heat loss.

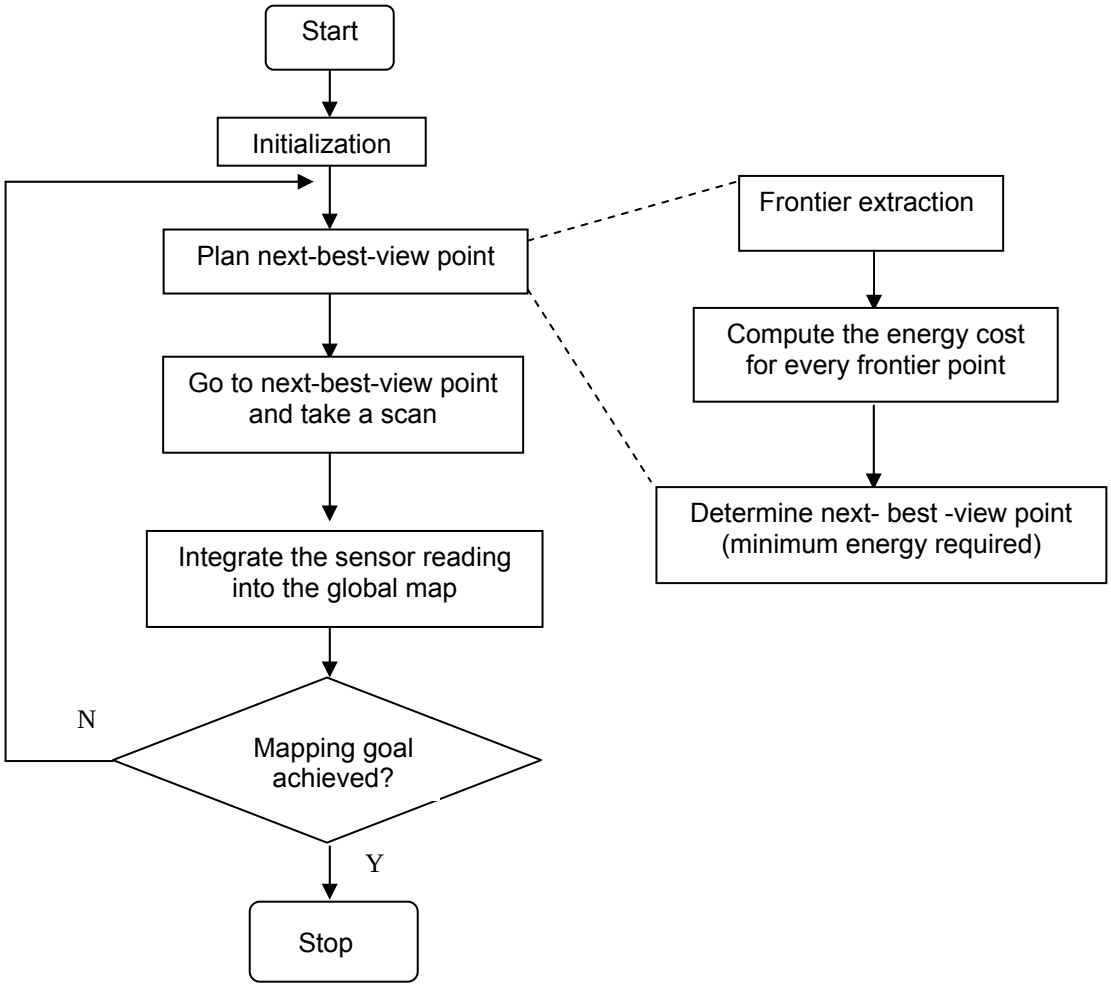


Figure 3. Next-best-view algorithm flow diagram.

### 4.2 Greedy method

The use of a triangular mesh to represent terrain allows the use of a graph search to easily find the next-best-view point. The triangular mesh map is stored in the computer as a directed weighted graph. Once the graph is constructed, an optimal path between the current rover location and a destination can be planned by Dijkstra's shortest path algorithm (Cormen et al. 2001). The objective of the greedy approach is to find an optimal path to minimize the traveling cost.

To start, the robot extracts the frontiers (Yamauchi 1997) from the triangles near the boundary of the current map, and then it constructs a voting scheme using the estimated energy cost for it to travel to frontiers. The robot visits the frontier with the minimum energy cost and takes a scan with its image sensor. The map is rebuilt by combining the new sensor reading. The robot plans the next-best-view point with the new map until it reaches the goal of exploration. Figure 3 shows the flow diagram of this greedy algorithm.

## 5. RESULTS

### 5.1 Algorithm validation

The efficiency of a mapping strategy is difficult to quantify, because map building is a complex task. Some researchers (Gonzalez-Banos and Latombe 2002; Taylor and Kriegman 1998; Thrun et al. 1998; Thrun et al. 2005) have shown the validity of algorithms by presenting paths generated to explore given environments. They validated algorithms by showing that the planner produces strategies that can not be easily out-done by a human operator (Gonzalez-Banos and Latombe, 2002). A few researchers (Moorehead et al. 2001; Sim and Dudek 2003; Stachniss and Burgard 2003; Sujan and Dubowsky 2005) opted to show the efficiency of proposed exploration strategies by comparing their results with other strategies.

In this paper, the performance of the greedy algorithm will be compared with the random method; the next-best-viewpoint is selected randomly within the frontiers of the environment. The comparison will show advantages of the intelligent greedy method over the random method without any intelligence.

### 5.2 Simulation Results

A simulated robot is placed in an unknown agricultural field of 800m by 800m as in Fig. 1, Indian Head Research Farm, Saskatchewan. The robot was assumed to have a 3D image sensor (with 90° field of view, 50 m depth of field, 1:1 aspect ratio) is installed on the robot as our vision system. The image sensor can rotate 360° horizontally.

The robot started near the lower left corner of the field (20,300). The exploration continued in the agricultural field until all reachable terrain was explored or expected new terrain information was negligible.

Captured intermediate screenshots of the simulation are shown in Fig. 4, where the traveled path (black lines) and updated map (white parts are explored terrain) are plotted at selected iteration times.

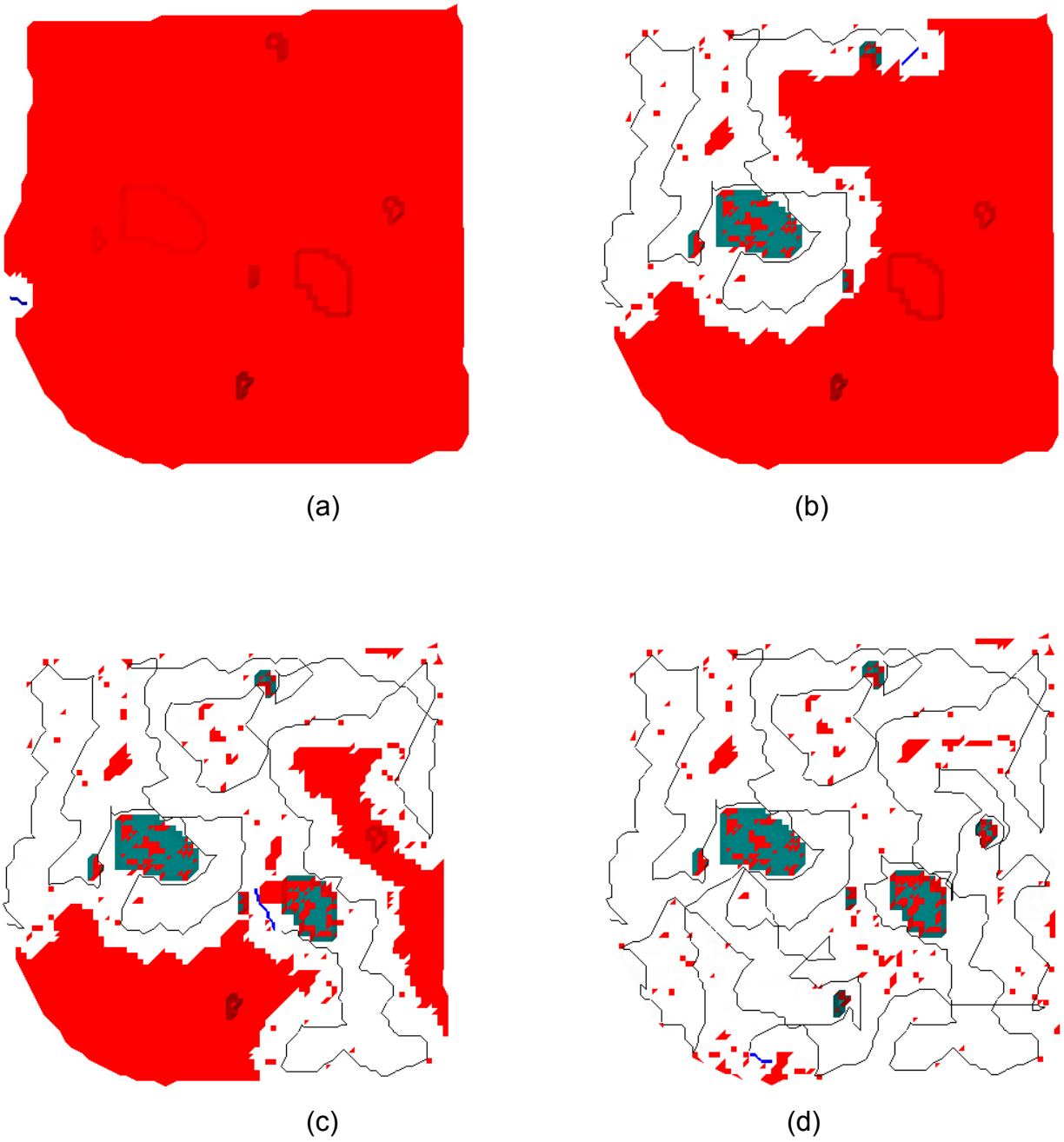


Figure 4. The traveled path (black lines) and updated map (white parts are explored terrain) are plotted at selected iteration times: (a) initialization; (b) after 70 iterations; (c) after 140 iterations; (d) after 208 iterations.

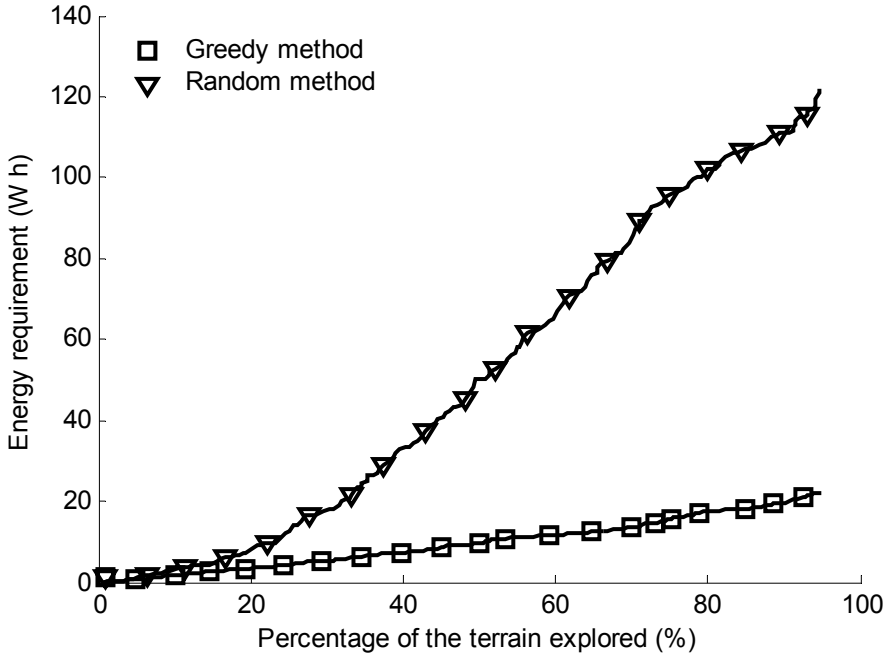


Figure 5. Result of the autonomous construction of an agricultural field map: energy requirement of the exploration as a function of fraction of explored terrain.

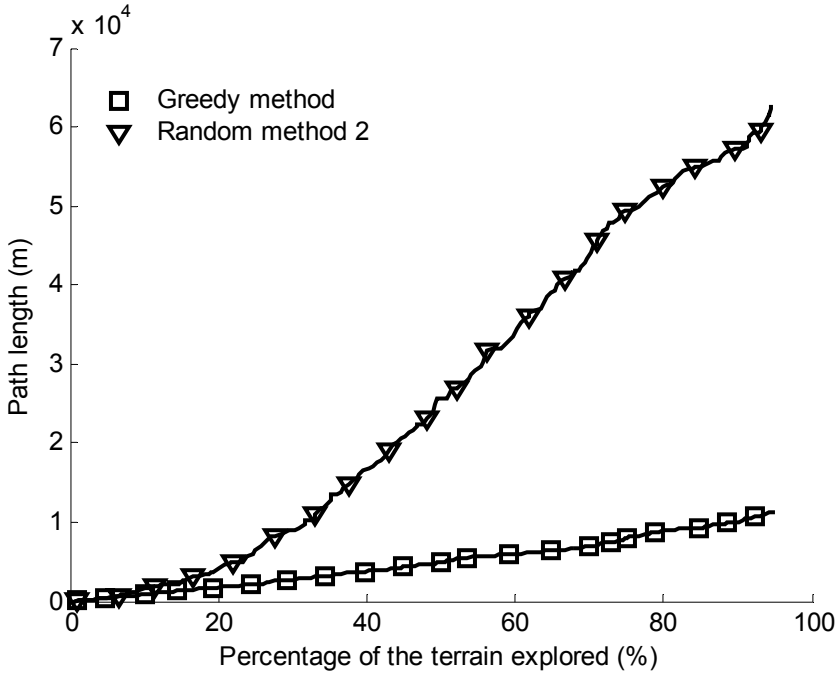


Figure 6. Result of the autonomous construction of an agricultural field map: path length traveled by the robot as a function of fraction of explored terrain.

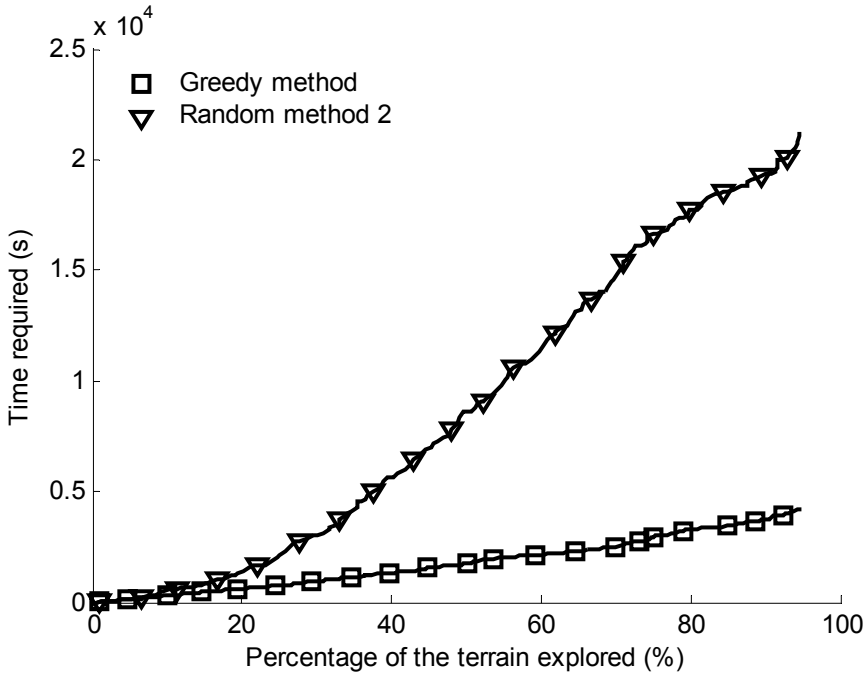


Figure 7. Result of the autonomous construction of an agricultural field map: time required of the exploration as a function of fraction of explored terrain.

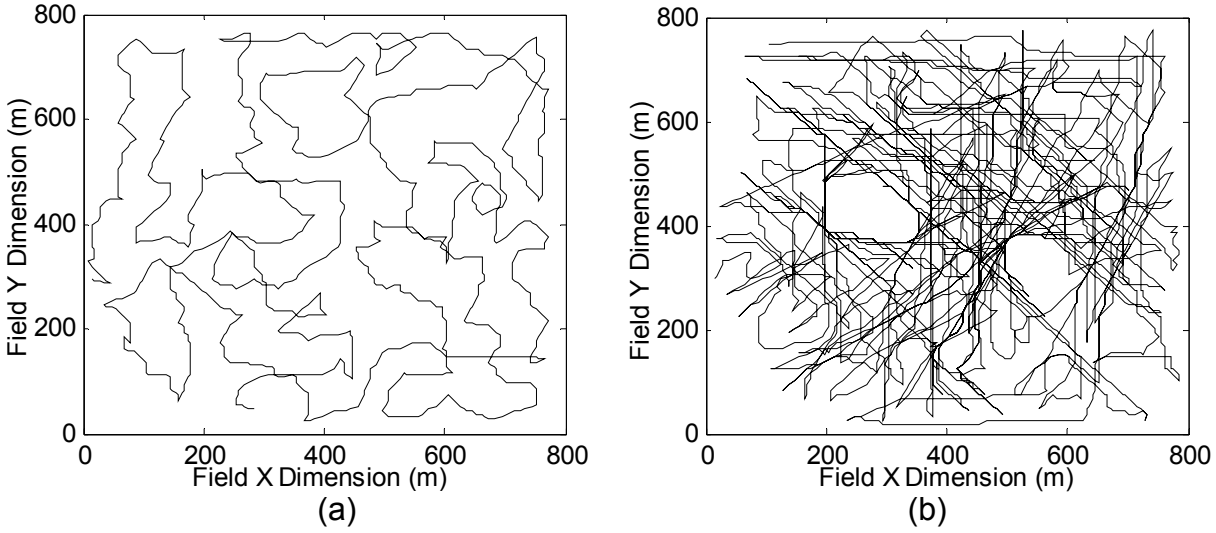


Figure 8. Trajectory generated in the simulation: (a) greedy method; (b) random method.

Figures 5-7 show the relationship of the fraction of the environment mapped and the energy requirement, the distance traveled and time requirement (including planning time and navigation time) by the robot for the 2 exploration strategies. It is desirable to have a

large fraction of the environment mapped with small energy consumption, short traveled distance, and short time. It is apparent that path length, energy requirement, and time requirement (including both the planning time and traveling time) of the greedy method are substantially smaller than those for the random method, whereas the fraction of the terrain explored is greater in the former. These results show a stark contrast between the 2 methods and illustrate the effectiveness of the greedy method in its ability to minimize energy demand during exploration. Figure 8 shows the comparison of the trajectory path generated from the greedy method and the random method.

## 6. CONCLUSIONS

In this paper we address the problem of autonomous mapping in large unstructured agricultural environments. A new triangular mesh map is presented that allows the robot to maintain a very rich representation of the environment, and to robustly perform exploration. A viewing frustum model and ray casting algorithm were described to facilitate the 3D image sensor simulation. Finally, the problem was addressed with the development of a novel next-best-view algorithm to map an unknown rough agricultural environment based on the energy cost function. To support this approach, a means for estimating the energy cost by considering the distance, terrain elevation change, vehicle slip rate, and other vehicle parameters was developed. This approach was applied to the next-best-view algorithm.

Experimental results in a typical western Canadian agricultural field are presented to demonstrate the algorithm. The resulting triangular mesh map can be used for different purposes such as obstacle avoidance, path planning, or other task planning related work.


### Acknowledgments

The authors acknowledge support from the Canadian Space Agency (CSA) and the Natural Sciences and Engineering Research Council (NSERC). Special note goes to Dr. J. Bakambu for his help with triangular mesh map building and Mr. P. Allard for help with the path planning. Dr. E. Dupuis provided valuable advice for this work. The authors also acknowledge the help of Dr. Guy Lafond, Agriculture and Agri-Food Canada, for providing GPS data of the field map used in this work.


### Reference


Åstrand, B., and A. Baerveldt. 2002. An Agricultural Mobile Robot with Vision-Based Perception for Mechanical Weed Control. In *Automatic Robots* 13: 21-35.

Bourgault, F., A.A. Makarenko, S.B. Williams, B. Grocholsky, and H.F. Durrant-Whyte. 2002. Information Based Adaptive Robotic Exploration. In *IEEE/RSJ International Conference on Intelligent Robots and Systems* 1*:* 540- 545. Lausanne, Switzerland. September 30 –October 5.

Choset, H. 2001. Coverage for robotics - A survey of recent results. In *Annals of Mathematics and Artificial Intelligence* 31: 113-126.

Cormen H.T., C.E. Leiserson, R.L. Rivest, and C. Stein. 2001. *Introduction to Algorithms*, Second Edition. MIT Press and McGraw-Hill.

Dupuis, E., P. Allard, J. Bakambu, T. Lamarche, and W.H. Zhu. 2004. Towards autonomous long-range navigation. In *8th ESA Workshop on Advanced Technologies for Robotics and Automation 'ASTRA 2004'*, ESTEC. Noordwijk, The Netherlands. November 2-4.

Gonzalez-Banos, H.H. and J.C. Latombe. 2002. Navigation strategies for exploring indoor environments. International Journal of Robotics Research 21(10-11): 829-848.

Hearn, D. 1994. Computer Graphics. Prentice-Hall. EngleWood Cliffs, New Jersey.

Hert, S., S. Tiwari, and V. Lumelsky. 1996. A terrain covering algorithm for an AUV. *Autonomous Robots* 3: 91-119.

Huang, W. 2001. Optimal line-sweep-based decompositions for coverage algorithms. In Proceedings of the 2001 IEEE International Conference on Robotics and Automation 27- 32. Seoul, Korea. May 21-26.

Keicher, R., and H. Seufert. 2000. Automatic guidance for agricultural vehicles in Europe. In *Computers and Electronics in Agriculture* 25: 169-194.

Kitware inc. 2005. The Visualization Toolkit. In *http://www.vtk.org*. Accessed June 26, 2005. New York.

Liljedahl, J. B., P.K. Turnquist, D.W. Smith, and M. Hoki. 1989. Tractors and Their Power Units. Van Nostrand Reinhold. New York.

Moorehead, S., R. Simmons, and W.L. Whittaker. 2001. Autonomous Exploration Using Multiple Sources of Information. In *Proceedings of the IEEE International Conference on Robotics and Automation* 3: 3098- 3103. May 21-26.

Nielsen, K.M., P. Andersen, T.S. Pedersen, T. Bak, and J.D. Nielsen. 2002. Control of an Autonomous Vehicle for Registration of Weed and Crop in Precision Agriculture. In *Proceedings of the IEEE Conference on Control Applications CCA/CACSD 2002*, Glasgow Scotland. September 18-20.

Ollis, M. and A. Stentz. 1996. First results in vision-based crop line tracking. In *Proceedings of the IEEE Robotics and Automation Conference* 951–956. Minneapolis, MN. April 22-28.

Reid, J.F. and S.W. Searcy. 1987. Vision-based guidance of an agricultural tractor. In *IEEE Control Systems* 7 (12): pp. 39–43.

Reid, J. F., Q. Zhang, N. Noguchi, and M. Dickson. 2000. Agricultural automatic guidance research in North America. In *Computers and Electronics in Agriculture* 25: 155-167.

Schroeder, W., K. Martin, and B. Lorensen. 1996. The Visualization Toolkit: An Object-Oriented Approach to 3D Graphics. Prentice Hall PTR. Upper Saddle River, New Jersy.

Sim, R. and G. Dudek. 2003. Effective Exploration Strategies for the Construction of Visual Maps. In *Proceedings of the IEEE/RSJ Conference on Intelligent Robots and Systems (IROS)* 3224-3231. Las Vegas, NV. October 27-31.

Stachniss, C. and W. Burgard. 2003. Exploring Unknown Environments with Mobile Robots using Coverage Maps. In *Proceedings of the International Joint Conference on Artificial Intelligence(IJCAI)* 1127-1134. Acapulco, Mexico. August 9-15.

Sujan,V. A., and S. Dubowsky. 2005. Efficient Information-based Visual Robotic Mapping in Unstructured Environments. *The International Journal of Robotics Research* 24 (4): 275-293.

Suvinen, A., M. Saarilahti. and T. Tokola. 2003. Terrain Mobility Model and Determination of Optimal Off-Road Route. In *Proceedings of the 9th Scandinavian Research Conference on Geographical Information Science*: 251-259. Espoo, Finland. July 4-6.

Taylor, C. and D. Kriegman. 1998. Vision-based motion planning and exploration algorithms for mobile robots. *IEEE Trans. On Robotics and Automation* 14(3):147–427.

Tillett, N. D. and T. Hague. 1999: Computer-Vision-based Hoe Guidance for Cereals — an Initial Trial. In *Journal of Agricultural Engineering Research* 74(3): 225-236.

Thrun, S., D. Fox, and W. Burgard. 1998. A probabilistic approach to concurrent mapping and localization for mobile robots. In *Machine Learning* 31:29–53.

Thrun, S., S. Thayer. W. Whittaker, C. Baker, W. Burgard, D. Ferguson, D. Hähnel, M. Montemerlo, A. Morris, Z. Omohundro, C. Reverte, and W. Whittaker. 2005. Autonomous Exploration and Mapping of Abandoned Mines. *IEEE Robotics and Automation Magazine* 11(4): 79-91.

Wong, J.Y. 1978. Theory of Ground Vehicles, John Wiley & Sons. New York; Toronto.

Yamauchi, B. 1997. A Frontier-Based Approach for Autonomous Exploration. In *Proceedings of the 1997 IEEE International Symposium on Computational Intelligence in Robotics and Automation* 146-151. Monterey, CA. July 10-11.